Catalytic Cysteine of Thymidylate Synthase Is Activated upon Substrate Binding[†,‡]

Jason Phan,[§] Elahe Mahdavian,[§] Michael C. Nivens,[§] Wladek Minor,[∥] Sondra Berger,[⊥] H. Trent Spencer,[▽] R. Bruce Dunlap,*[,§] and Lukasz Lebioda*[,§]

Departments of Chemistry and Biochemistry, Biological Sciences, and Basic Pharmaceutical Sciences, University of South Carolina, Columbia, South Carolina 92908, and Department of Molecular Physiology and Biological Physics, University of Virginia, Charlottesville, Virginia 22901

Received February 16, 2000; Revised Manuscript Received March 28, 2000

ABSTRACT: The role of Ser 167 of *Escherichia coli* thymidylate synthase (TS) in catalysis has been characterized by kinetic and crystallographic studies. Position 167 variants including S167A, S167N, S167D, S167C, S167G, S167L, S167T, and S167V were generated by site-directed mutagenesis. Only S167A, S167G, S167T, and S167C complemented the growth of thymidine auxotrophs of *E. coli* in medium lacking thymidine. Steady-state kinetic analysis revealed that mutant enzymes exhibited k_{cat} values 1.1−95-fold lower than that of the wild-type enzyme. Relative to wild-type TS, K_m values of the mutant enzymes for 2′-deoxyuridylate (dUMP) were 5−90 times higher, while K_m values for 5,10-methylenetetrahydrofolate (CH_2H_4folate) were 1.5−16-fold higher. The rate of dehalogenation of 5-bromo-2′-deoxyuridine 5′-monophosphate (BrdUMP), a reaction catalyzed by TS that does not require CH_2H_4folate as cosubstrate, by mutant TSs was analyzed and showed that only S167A and S167G catalyzed the dehalogenation reaction and values of k_{cat}/K_m for the mutant enzymes were decreased by 10- and 3000-fold, respectively. Analysis of pre-steady-state kinetics of ternary complex formation revealed that the productive binding of CH_2H_4-folate is weaker to mutant TSs than to the wild-type enzyme. Chemical transformation constants (k_{chem}) for the mutant enzymes were lower by 1.1−6.0-fold relative to the wild-type enzyme. S167A, S167T, and S167C crystallized in the $I2_13$ space group and scattered X-rays to either 1.7 Å (S167A and S167T) or 2.6 Å (S167C). The high-resolution data sets were refined to a R_{crys} of 19.9%. In the crystals some cysteine residues were derivatized with 2-mercaptoethanol to form *S*,*S*-(2-hydroxyethyl)thiocysteine. The pattern of derivatization indicates that in the absence of bound substrate the catalytic cysteine is not more reactive than other cysteines. It is proposed that the catalytic cysteine is activated by substrate binding by a proton-transfer mechanism in which the phosphate group of the nucleotide neutralizes the charge of Arg 126′, facilitating the transfer of a proton from the catalytic cysteine to a His 207−Asp 205 diad via a system of ordered water molecules.

Thymidylate synthase (TS),[1] the enzyme that catalyzes the reductive methylation of dUMP to thymidine monophosphate (dTMP) with the cofactor CH_2H_4folate as a one-carbon donor and a reducing power source, has been a primary target for cancer chemotherapy and gene therapy. Although the physical structure of TS has been relatively well defined and its complex catalytic mechanism thoroughly studied, many aspects of TS catalysis remain challenging questions. A precise orientation of the substrate and cofactor molecules in the active site is required for a catalytically competent TS enzyme. Among numerous highly conserved residues in TS from different species are 11 residues that are directly involved in binding ligands in the reaction site (*1*, *2*). Ser 167 in *Escherichia coli* TS (ecTS), corresponding to Ser 216 in human TS (hTS) and Ser 219 in *Lactobacillus casei* (lcTS), is highly conserved, since only one of 29 TSs from different species has a residue other than Ser in this position (*3*).

Mutagenesis of the human colorectal tumor cell line C led to the isolation and characterization of a TS-deficient

[†] This work was supported by NIH Grants CA 76560 and CA 78651. Some instrumentation used in this research was purchased with NSF Grant BIR 9419866 and DOE Grant DE-FG-95TE00058. Use of the Argonne National Laboratory Structural Biology Center beamlines at the Advanced Photon Source was supported by the U.S. Department of Energy, Office of Science, under Contract W-31-109-ENG-38.

[‡] The PDB files of the crystal structures of mutant TSs S167A, S167T, S167T reduced, and S167C were deposited in the Protein Data Bank as entries 1ev5, 1evf, 1evg, and 1ev8, respectively.

* To whom correspondence should be addressed at the Department of Chemistry and Biochemistry, University of South Carolina, 730 S. Main St., Columbia, SC 29208. Phone (803) 777-2140; fax (803) 777-9521; e-mail lebioda@psc.sc.edu.

[§] Department of Chemistry and Biochemistry, University of South Carolina.

[∥] University of Virginia.

[⊥] Department of Basic Pharmaceutical Sciences, University of South Carolina.

[▽] Department of Biological Sciences, University of South Carolina.

[1] Abbreviations: TS, thymidylate synthase; dUMP, 2′-deoxyuridine 5′-monophosphate; dTMP, thymidine 5′-monophosphate; CH_2H_4folate, 5,10-methylenetetrahydrofolate; ecTS, *Escherichia coli* thymidylate synthase; lcTS, *Lactobacillus casei* thymidylate synthase; hTS, human thymidylate synthase; FdUMP, 5-fluoro-2′-deoxyuridine 5′-monophosphate; EDTA, ethylenediaminetetraacetic acid; 2-ME, 2-mercaptoethanol; IPTG, isopropyl β-D-thiogalactopyranoside; DTT, dithiothreitol; BrdUMP, 5-bromo-2′-deoxyuridine 5′-monophosphate; DTNB, 5,5′-dithiobis(2-nitrobenzoic acid); Tris, tris(hydroxymethyl)aminomethane; H_4folate, (+)-tetrahydrofolate; PCR, polymerase chain reaction; CFE, cell-free extract; PDB, Protein Data Bank.

10.1021/bi000367g CCC: $19.00 © 2000 American Chemical Society
Published on Web 05/12/2000

subline denoted C18 (*4*). Analysis of TS cDNA from C18 cells revealed a single mutation that predicts the replacement of Ser 216 (Ser 167 in ecTS) by a leucine residue. Subsequently, 12 mutant hTSs with substitutions at position 216 were created for studies of the function of Ser 216, of which only S216T was able to complement the growth of a TS-deficient *E. coli* strain (*5*). This led to a hypothesis that the serine residue is involved not only in substrate binding but also in TS catalysis. It was proposed that Ser216 is involved in a proton relay mechanism that serves to activate the catalytic cysteine. In the proposed mechanism, a proton is transferred from the thiol to invariant His 256 (His207, ecTS), which functions as a general base (Williams et al., unpublished data). Prompted by this hypothesis, we studied the kinetics and crystal structures of mutant enzymes from ecTS with substitutions at position 167 and report here the results.

EXPERIMENTAL PROCEDURES

Materials. dUMP, TMP, FdUMP, ethylenediaminetetraacetic acid (EDTA), 2-mercaptoethanol (2-ME), isopropyl β-D-thiogalactopyranoside (IPTG), dithiothreitol (DTT), 5-bromo-2′-deoxyuridylate (BrdUMP), and 5,5′-dithiobis(2-nitrobenzoic acid) (DTNB) were obtained from Sigma (St. Louis, MO). Tris(hydroxymethyl)aminomethane (Tris) was from Research Organics, Inc. (Cleveland, OH). Formaldehyde was purchased from Fisher (Pittsburgh, PA). Ultrapure ammonium sulfate was from ICN Biomedicals, Inc. (Aurora, OH). Oligonucleotides utilized for site-directed mutagenesis were purchased from Integrated DNA Technologies, Inc. (Coralville, IA). Centricon concentrators were obtained from Millipore Corp. (Bedford, MA). (+)-Tetrahydrofolate (H_4folate) was prepared by the enzymatic reduction of folic acid by *Lactobacillus casei* dihydrofolate reductase and was converted to CH_2H_4folate by the addition of a 20-fold molar excess of formaldehyde.

Enzyme Expression and Isolation. The gene encoding wild-type ecTS, a gift from Dr. Dallas (Glaxo Wellcome), was PCR-amplified to include *Xba*I and *Cla*I restriction sites immediately before and after the coding region, respectively, and cloned into the *Xba*I and *Cla*I sites of constitutive vector pBluescript SK (Stratagene). Construction of wild-type and Ser 167 variants of ecTS was carried out by site-directed mutagenesis by the overlap extension method (*6*). Following mutagenesis, cDNA of wild-type or variant ecTS was transformed into P2913, a TS^- strain of *E. coli*, by the $CaCl_2$/heat shock method (*7*). Ampicillin-resistant colonies were obtained and mutations were confirmed by dideoxy DNA sequencing of the PCR amplified regions. Overnight cultures (10 mL) of X2913 cells containing the various plasmids were grown in Luria broth and used to inoculate 1-L cultures containing 100 μg/mL ampicillin. After 12−16 h of incubation, cells were pelleted by centrifugation at 5000*g* for 30 min. Wild-type and mutant enzymes were purified by Q-Sepharose chromatography on a FPLC system equipped with LCC 500 controller (Pharmacia). All purification steps were performed at 4 °C. The chromatographic buffers used were QA [50 mM Tris (pH 7.5), 14 mM 2-ME, and 1 mM EDTA] and QB [50 mM Tris (pH 7.5), 1 M KCl, 14 mM 2-ME, and 1 mM EDTA]. Purification buffers were filtered with 40 μm membranes (Gelman, Ann Arbor, MI), and degassed with helium for 10 min prior to the addition of 14 mM 2-ME. A cell-free extract (CFE) was obtained from 2 g of wet cells treated with five 30-s consecutive cycles of sonication (Branson sonifier 450) in 25 mL of degassed QA buffer and then centrifuged at 11000*g* for 30 min. The CFE was applied to a 2.5 cm × 20 cm Q-Sepharose column that had been equilibrated with QA buffer, and a linear gradient of 20−60% QB was used for enzyme elution. Fractions were monitored spectrophotometrically, and wild-type and mutant enzymes typically eluted at 36−42% QB (360−400 mM KCl) buffer. Purified protein was stored in 15% glycerol at −70 °C. Enzyme purity was assessed by SDS−PAGE.

Spectrophotometric Assay. Enzyme activity was determined by measuring the formation of dihydrofolate, which was monitored at 340 nm after addition of enzyme to the reaction assay (*8*). Measurements were made at pH 7.5 and 27 °C in Morrison buffer [100 mM Tris, 50 mM 2-(*N*-morpholino)ethanesulfonic acid, and 50 mM acetic acid] (*9*). One unit of enzyme activity is defined as the amount of enzyme that produces 1 μmol of TMP/min at 27 °C. Enzyme concentration was determined by measurement of absorbance at 280 nm, as described previously (*10*). The values of k_{cat} and K_m were determined by the procedure described previously (*11*). Data were collected with a Hewlett-Packard 8450A UV−vis spectrophotometer.

Growth Complementation Analysis. To investigate the in vitro growth effects of mutation at position 167 of ecTS, P2913 transformants containing wild-type and mutant enzymes were grown overnight in minimal medium [12% casamino acids, Met, Leu, His, Thr, and Lys (each 5 mg/mL), KH_2PO_4 (15 mM), NaH_2PO_4 (35 mM), sodium citrate (1.7 mM), $MgSO_4$ (0.4 mM), $(NH_4)SO_4$ (7.5 mM), and 40% glucose] containing 100 μg/mL Amp in the presence and absence of thymidine. Minimal medium cultures (10 mL) were then diluted 1:1000 into minimal medium in the presence and absence of thymidine (200 μg/mL), and the absorbance at 600 nm was measured over 12 h.

Enzyme Kinetics. To determine the K_m(dUMP) for wild-type and Ala 167 ecTS, varying concentrations of dUMP (0−100 μM) were used with constant concentrations of enzyme (30 nM) and CH_2H_4folate (100 μM). The K_m(dUMP) values for the other mutants were obtained in the same manner with a range of dUMP concentrations (0−800 μM) at constant concentrations of enzyme (1−300 μM) and CH_2H_4folate (0.4−1 mM). The values of K_m(CH_2H_4folate) for wild-type and Ala 167 TSs were determined with varying concentrations of CH_2H_4folate (0−100 μM) at constant concentrations of enzyme (30 nM) and dUMP (100 μM). For the other variants, concentrations of CH_2H_4folate ranging from 0 to 800 μM were used with constant concentrations of enzyme (0.3−1 μM) and dUMP (0.4−1 mM). The pre-steady-state kinetic constants k_{iso}, $k_{r,iso}$, k_{chem}, and K_d(CH_2H_4-folate) for wild-type and mutant TSs were obtained with a final enzyme concentration of 2 μM, a saturating concentration of dUMP (1 mM), and varying concentrations of CH_2H_4-folate (10−150 μM). Ligand binding was analyzed by stopped-flow fluorescence spectroscopy on an Applied Photophysics spectrophotometer as described by Spencer et al. (*12*). Typically, a final enzyme concentration of 3 μM and varying concentrations of dUMP and FdUMP (0−500 μM) were used to determine the association (k_{on}) and dissociation (k_{off}) constants for binary complex formation at two different temperatures (5 and 20 °C).

TS-Catalyzed Dehalogenation of BrdUMP. Catalytic debromination of BrdUMP by TS was monitored spectrophotometrically at 25 °C by the decrease in absorbance accompanying debromination ($\Delta\epsilon_{285} = 5320\ M^{-1}\ cm^{-1}$) (*11*). The reaction mixture (900 μL) contained Morrison buffer, 10 mM DTT, BrdUMP (0−200 μM for wild-type TS; 0−400 μM for S167A; 0−2.5 mM for S167G), and 3−5 μM enzyme. Absorption data were fitted to the Michaelis−Menten equation by the Kaleidagraph 3.01 program on a Macintosh Quadra 650, and the values of k_{cat} and K_m were determined.

Reaction of TS Sulfhydryl Groups with DTNB. Reaction of sulfhydryl groups with DTNB yields 2-nitro-5-thiobenzoate, the formation of which is monitored at 412 nm ($\Delta\epsilon_{412} = 13\,600\ M^{-1}\ cm^{-1}$) (*13*). Exogenous 2-ME from purified enzymes was removed by gel filtration prior to reaction (*14*). The final reaction mixture contained 0.5 mg/mL EDTA, 500 μM DTNB in 0.1 M phosphate buffer at pH 7.4, and approximately 5 μM enzyme. The increase in absorbance was measured on a Shimadzu UV-2101PC scanning spectrophotometer.

Crystallization of S167 Variant TSs. Crystals were grown by the vapor diffusion method in the hanging drop setup at room temperature (*15*). Typically, 5 μL of enzyme solution (7−10 mg/mL) containing 1 mM EDTA, 15 mM 2-mercaptoethanol, 50−100 mM potassium chloride, and 20−50 mM potassium phosphate (pH 7.5) was mixed with an equal volume of precipitant solution containing either 48% saturated ammonium sulfate, 20 mM 2-ME, and 100 mM Tris-HCl (pH 7.8) (S167A, S167T) or 68% saturated ammonium sulfate, 100 mM potassium phosphate (pH 8.5), and no reducing agent (S167C), and the mixture was allowed to equilibrate with 0.6 mL of precipitant solution present in the well. Crystals appeared after 3 weeks and grew to the size of 0.1−0.5 mm within 1 week.

X-ray Diffraction Data Measurement and Processing. The crystals of S167A and S167T TSs, measuring approximately 0.35 × 0.35 × 0.35 and 0.15 × 0.15 × 0.15 mm, respectively, were transferred to a cryoprotectant solution, 45% saturated ammonium sulfate, 30% ethylene glycol, and 0.1 M Tris, pH 7.8, and flash-cooled in liquid nitrogen. Crystallographic diffraction experiments were carried out at the SBC insertion device beamline of the advanced photon source at Argonne National Laboratory with X-rays of 0.9793 Å in wavelength. The data were collected at a crystal to detector distance of 150 mm and indexed, integrated, and scaled with the HKL 2000 suite of programs (*16*). A crystal of S167C and a second, "reduced" crystal of S167T TS, each measuring 0.15 × 0.15 × 0.15 mm, were flash-cooled in N_2 vapors (at −178 °C generated with a Molecular Structure Corp. X-Stream low-temperature attachment) and used for data collection with Cu Kα radiation by an R-Axis IV area detector with Yale mirrors and Rigaku RU 200 rotating anode source operating at 50 kV and 100 mA. The "reduced" crystal of S167T TS was grown and maintained under reducing conditions by adding 2-ME to the well every 4 days. Prior to diffraction, it was transferred to a fresh solution of 2-ME and to a cryogen containing 20 mM 2-ME. The Cu Kα data were processed with HKL (*16*). The structure of wild-type ecTS (PDB code 1tjs; *17*) with the appropriate amino acid sequence modifications was used as the starting model in molecular replacement for Ala 167 TS with AMORE (*18*) from the CCP4 software suite (*19*). The data were initially refined with automated procedures in the ARP/wARP suite of programs (*20*) and optimized with the CNS software (*21*) by use of positional and temperature refinements. Electron density maps calculated with $2F_o-F_c$, and F_o-F_c coefficients were utilized to introduce manual corrections to the model with the interactive graphics program CHAIN (*22*). For the other structures reported here, the refined structure of S167A TS was used as the starting model in the crystallographic refinements utilizing CHAIN for model rebuilding and CNS for model optimization.

RESULTS

Growth Complementation of TS-Deficient E. coli. A TS-deficient strain of *E. coli*, X2913, was transformed with plasmids encoding wild-type and mutant TSs. Analysis of growth rates of X2913 transformants was conducted in the presence and absence of exogenous thymidine. As expected, *E. coli* X2913 expressing wild-type or mutant enzymes grew in medium supplemented with 200 μg/mL thymidine. The growth rates of all transformants were similar over a 12 h period. Transformants expressing wild-type enzyme, S167A, S167C, S167G, and S167T exhibited similar growth rates in medium lacking thymidine (data not shown). In contrast, X2913 transformants expressing S167D, S167L, S167N, and S167V were unable to grow in medium lacking thymidine (data not shown). All Ser 167 mutants expressed similar levels of TS in the cell-free extract as observed in SDS−PAGE (data not shown). Thus, the inability of the mutants (Asn, Asp, Leu, and Val) to support growth of a TS-deficient bacterial strain in the absence of thymidine is due to a defect in the enzyme and not a lack of TS expression.

Generation and Isolation of S167 Variants. Cell-free extracts from transformants expressing wild-type and the four complementing mutant enzymes contained TS expressed at a level of approximately 15% of the total cellular protein as judged by SDS−PAGE. In all cases, the amount of insoluble TS protein in the cell paste was negligible. Wild-type and mutant TSs were purified by a single anion-exchange Q-Sepharose column. Typically, from 2 g of wet cells, 63−85% of total TS was recovered with a 6.0−10-fold purification. The purity of each enzyme was confirmed by SDS−PAGE as a single band at ∼35 kDa.

Analysis of Kinetic Properties of Variant TSs. Steady-state kinetic parameters (k_{cat}, K_m) were obtained for wild-type TS and complementing mutants (Table 1). Values of k_{cat} and K_m for both nucleotide and cofactor were determined from the Michaelis−Menten plot of velocity versus substrate concentration. The K_m values for dUMP were increased by 5-fold for S167A, 30−38-fold for S167G and S167T, and about 90-fold for S167C, relative to that for wild-type enzyme. The K_m values for CH_2H_4folate were not significantly increased for S167A (1.4-fold) but were 5−8-fold higher for S167G and S167T and about 16-fold higher for S167C. The k_{cat} values were decreased slightly for S167A but were 5-, 6-, and 95-fold lower for S167G, S167T, and S167C, respectively. More importantly, at saturating concentrations of CH_2H_4folate, the k_{cat}/K_m values for dUMP were decreased by 5.3-fold for S167A, 165-fold for S167G, 250-fold for S167T, and ∼9000-fold for S167C. The k_{cat}/K_m values for CH_2H_4folate at saturating concentrations of dUMP for S167A, S167G, and S167T were decreased by 2−50-fold and by 1500-fold for S167C.

Table 1: Steady-State Parameters for S167 Variants[a]

ecTS	K_m for dUMP (μM)	K_m for CH_2H_4folate (μM)	k_{cat} (s^{-1})	k_{cat}/K_m (dUMP)	k_{cat}/K_m (CH_2H_4folate)
wild type	1.1	8.1	2.1	1.9	0.3
S167A	5.3	12.0	1.9	0.4	0.2
S167G	33.9	42.4	0.39	0.01	0.009
S167T	41.7	62.7	0.32	0.008	0.005
S167C	98.1	130	0.022	0.0002	0.0002

[a] Experiments were repeated a minimum of three times. All standard deviations are within 10% of the reported values except for the k_{cat} of S167C, which is 18%.

Table 2: Pre-Steady-State Kinetic Parameters for CH_2H_4folate Binding to S167 Variants[a]

ecTS	k_{iso} (s^{-1})	$k_{r,iso}$ (s^{-1})	k_{chem} (s^{-1})	K_d (10^{-6} M)	[a]K_m (CH_2H_4folate) (10^{-6} M)
wild type	70	8.5	2.0	65	8.5
S167A	65	9.0	1.9	68	9.7
S167G	11	9.5	0.40	90	42.6
S167T	8.5	10.0	0.33	95	52.1

[a] For each stopped-flow experiment, at least 5 traces were averaged for each CH_2H_4folate concentration and each experiment was repeated a minimum of three times. The standard deviations are within 15% of the reported values.

Pre-Steady-State Analysis of CH_2H_4folate Binding to ecTS-dUMP. Nucleotide binding to wild-type ecTS induces quenching of tryptophan fluorescence, the rate of which can be used to calculate rate constants governing nucleotide binding. The amplitude of fluorescence quenching upon nucleotide binding to the S167 variants was not sufficient for accurate determinations of rate constants governing nucleotide binding, but fluorescence quenching upon ternary complex formation was easily observed. The binding of CH_2H_4folate to ecTS at saturating concentrations of dUMP leads to the formation of the ternary complex, which undergoes a conformational change to form a closed structure. This is followed by chemical transformation of bound substrate to bound product. The kinetic constants that define these steps, k_{iso}, $k_{r,iso}$, k_{chem}, and K_d, are shown in Table 2. The k_{iso} values were decreased slightly (1.1-fold) for S167A and significantly (6−8-fold) for S167G and S167T, relative to that of wild-type TS. Although values of $k_{r,iso}$ were similar among the enzymes, a slightly faster rate of reverse isomerization is observed for mutant enzymes. The values of k_{chem} were 1.1−6-fold slower than that of wild-type enzyme and are consistent with the k_{cat}s determined by steady-state analysis. The higher K_ds for CH_2H_4folate suggest that initial binding of CH_2H_4folate to the binary complex is moderately impaired in mutant TSs. The values of K_m for CH_2H_4folate calculated from transient-state analysis are in good agreement with those from the Michaelis−Menten treatment of steady-state kinetic data (Tables 1 and 2).

Dehalogenation of BrdUMP. In the presence of exogenous thiols, TS catalyzes the dehalogenation of BrdUMP to yield dUMP, Br^-, and a disulfide (*11*). It is postulated that the catalytic Cys 198 of lcTS adds to C-6 of BrdUMP to form the 5-bromo-5,6-dihydropyrimidine intermediate. Reaction of the dihydropyrimidine intermediate with exogenous thiol is postulated to lead to the formation of an enolate intermediate. The latter undergoes β-elimination to give dUMP. Wild-type and mutant TSs with small hydrophobic side chains (S167A and S167G) catalyzed the thiol-dependent dehalogenation of BrdUMP to dUMP (Table 3). Relative to wild-type TS, the k_{cat} values of S167A and S167G were decreased by 1.2- and 50-fold, and the K_m values increased 7.0- and 53-fold, respectively. No debromination of BrdUMP was detected with concentrations of S167T or S167C of 5 μM in the presence of 500 μM BrdUMP in reactions proceeding for 2 h. S167A had a 1.2-fold lower k_{cat} and a 7-fold higher K_m for debromination than wild-type TS.

Table 3: Rate of Dehalogenation Catalyzed by S167 Variants[a]

ecTS	K_m for BrdUMP (μM)	k_{cat} (s^{-1})	k_{cat}/K_m
wild type	9.7	0.099	0.010
S167A	72.3	0.078	0.0011
S167G	514	0.0019	0.0000036

[a] Each experiment was performed a minimum of three times. The standard deviations for wild type and S167A are within 10% of the reported values but are approximately 25% for S167G.

Determination of Sulfhydryl Contents of Wild Type and S167 Variants. DTNB reacts with aliphatic thiol compounds to produce 1 mol of *p*-nitrothiophenol anion/mol of thiol (*13*). The DTNB reaction with sulfhydryl groups of TS was monitored by observing the increase in absorbance due to the formation of the *p*-nitrophenol anion ($\Delta\epsilon_{412}$ = 13 600 M^{-1} cm^{-1}). Wild-type ecTS has five cysteine residues per subunit while S167C has six cysteine residues per subunit. Prior to reaction with DTNB, exogenous thiol was removed from the enzymes by gel filtration. The number of sulfhydryl groups for the wild-type enzyme was determined to be 3.9 per subunit and the number of sulfhydryl groups for S167C mutant was 4.0 per monomer, in agreement with the crystallographic data (see below). Incubation of S167C under denaturing and reducing conditions (8 M urea, 100 mM DTT) followed by dethiolation and reaction with DTNB revealed that the mutant enzyme contained 6.0 sulfhydryl groups per monomer in the denatured form.

Structural Analysis of S167 Variants. All three mutants crystallized in the space group $I2_13$ with one subunit in the asymmetric part of the unit cell. The parameters and statistics of crystallographic refinements are summarized in Table 4. The initial model was, in general, excellent; however, some side chains were rebuilt to fit to the more resolved density and preferred rotamers (Table 5). S167A data, which were refined first, having a mosaicity of 0.31 and an overall R_{merge} of 0.056, yielded excellent electron density maps. Among other information, they revealed precisely the positions of main-chain carbonyl groups that are crucial in stabilizing the active-site β-bulge (*23*−*25*). The side chain of the active-site Cys 146 is disordered between two positions, one of which is more populated. The cryoconditions and high-resolution data resulted in well-resolved solvent structure. A chain of highly ordered water molecules forms an

Table 4: Crystallographic and Refinement Statistics

variant TSs	Ala167	Thr167	Thr167[a]	Cys167
X-ray source	synchrotron	synchrotron	Cu Kα	Cu Kα
space group (Å)	$I2_13$	$I2_13$	$I2_13$	$I2_13$
$a = b = c$	132.49	132.49	131.97	136.27
mosaicity (deg)	0.306	0.195	0.259	0.572
resolution (Å)	1.70	1.70	2.00	2.60
reflections, measured	459 585	406 122	271 787	136 184
reflections, independent	42 586	55 744	25 985	12 205
completeness (%)	99.9	99.8	99.8	93.0
R_{sym}[b]	0.056	0.085	0.083	0.125
R_{crys}[c]/R_{free}	0.19/0.21	0.19/0.21	0.21/0.22	0.22/0.26
average B (Wilson plot)	18.69	16.95	16.78	48.61
most favored ϕ/ψ (%)	90.0	90.9	90.4	84.3
rmsd, bond lengths (Å)	0.005	0.006	0.006	0.010
rmsd, bond angles (deg)	1.4	1.4	1.5	1.6
rmsd in Cα[d] (Å)	0.35	0.12	0.17	0.47
no. of solvent molecules	233	306	86	11
no. of ligand molecules	3	3	3	0

[a] Unmodified Cys146. [b] $R_{sym} = (\sum_h|I_h - \langle I\rangle|)/(\sum_h I_h)$. [c] $R_{crys} = (\sum_h|F_{obs} - F_{cal}|)/(\sum_h F_{obs})$. R_{free} = crystallographic R-factor for test set as implemented in CNS 0.5 (*21*). [d] Root-mean-square deviation for Ala167 TS Cα trace upon superposition on the initial model (1tjs); Ala167 structure was used as the reference for the other mutants.

Table 5: Rebuilt Side Chains, Disordered Residues, and Atoms Missing Density in the Final $2F_o - F_c$ Map Contoured at 1σ Level

Rebuilt Side Chains

Leu 5	Lys 48	Asn 76	Arg 127[a]	Asn 177	Ile 231[a]
Glu 6	Thr 51[b]	Thr 78	Val 130	Leu 184	Arg 243
Leu 7	Leu 52	Trp 83	Leu 138	Gln 191	Glu 245
Met 8	Arg 53	Pro 102[c]	Lys 140	Asp 214[b]	Pro 256[c]
Glu 14	Leu 60	Pro 104[c]	Leu 143[b]	Thr 216	Lys 259
Glu 17	Gln 64	Ile 112	Leu 163	Leu 218	Ala 260[a]
Lys 18[a]	Asp 66[a]	Leu 116	Gln 165	Leu 220	Pro 261[a]
Met 34	Thr 67	Lys 120	Arg 166	Ser 221	Ile 264
Gln 39	Ile 69[a]	Asn 121	Leu 172	Leu 230	

disordered residue	atoms missing density	*x*-fold disorder
Lys 2	ζ	
Thr 16		2
Ser 28		3
Val 45		2
Asp 20	N, α, β, C, O	
Arg 21	N, α, β, γ, δ, ϵ, ζ, η	
Thr 22	N, α, β, γ, δ, ϵ	
His 73	γ, $N_δ$, $C_δ$	
Glu 86	β, ϵ	
Lys 120	ζ	
Leu 143	δ	
Lys 233	ϵ, ζ	
Glu 237	γ, δ, ϵ	
Glu 248	δ, ϵ	
Ile 249		2
Lys 259	ζ	

[a] Main and side chains. [b] Main-chain only. [c] Position of Cγ only.

extensive hydrogen-bonding network in the immediate vicinity of Cys 146 (Figure 1, top). Starting at the site of mutation, water molecule W 67 is in contact with the Ala 167 $C_β$ (3.4 Å) and with Cys 146 $S_γ$ (2.7 Å). This water molecule is hydrogen-bonded to the ordered water W 192 (2.7 Å). The latter is not observed in the other mutant structures, which have a bulky side chain at position 167 or a poorly resolved solvent structure (S167C). Water W192 forms a hydrogen bond with the highly ordered water W100 (3.1 Å), which is observed in all mutants, and is stabilized by Arg 126′ (from the other subunit), His 207, and Tyr 94 (Figure 1, bottom). This hydrogen-bond system may serve to channel the proton from the catalytic sulfhydryl group of Cys 146 to His 207 (see Discussion).

In all structures the $N_δ$ of His 207 forms a hydrogen bond (2.8−3.2 Å) to the carboxylate of Asp 205 and the $N_ϵ$ to water molecule W100 (2.9 Å). The distance between the hydroxyl oxygen of Thr 167 and the $C_ϵ$ of His 207 is 3.4 Å, supporting the selected orientation of the imidazole. At a low contouring level, Cys 146 showed 2-fold disorder with one conformation similar to that of the other mutants and the initial model 1tjs. At a higher contouring level ($\sigma = 2.0$), a single dominant conformation rotated approximately 70° toward the carbonyl group of Ala 167 was observed. This orientation put Cys 146 $S_γ$ in contact with Ala 167 carbonyl oxygen and the amide oxygen of Glu 165 (Figure 2). This orientation is also observed in the "reduced" S167T structure as a partially occupied, minor conformation. In S167T

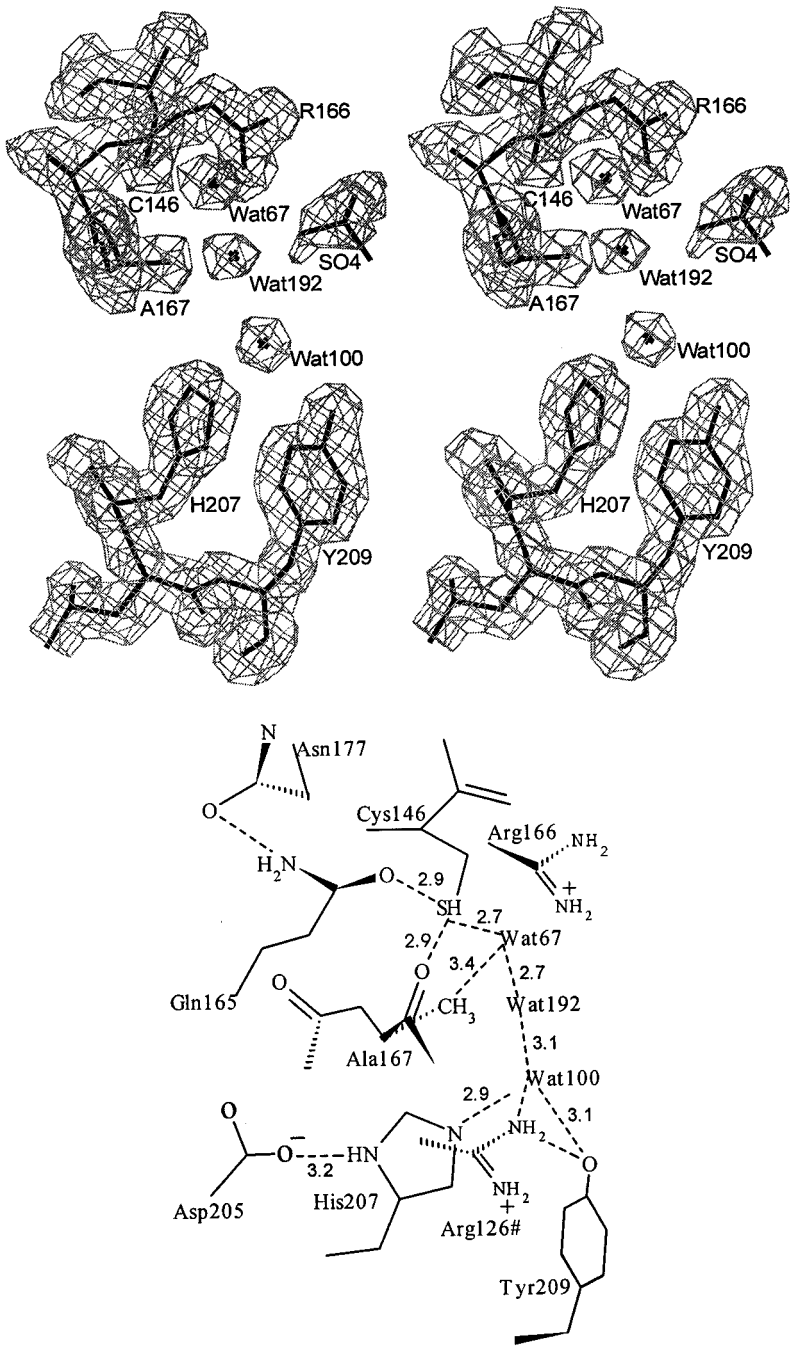

FIGURE 1: Active site of ecTS S167A with the chain of water molecules connecting Cys 146 to His 207. (Top) Stereoview of the electron density calculated with $2F_o-F_c$ coefficients and contoured at 1.0σ level. (Bottom) Scheme of hydrogen bonding with distances in angstroms.

structures, the side-chain hydroxyl group of Thr 167 occupies the same position as the hydroxyl of the serine in the wild-type protein, while the methyl group interferes with the positioning of water W67. Unlike in the other mutant structures, no density was present for a phosphate group in S167C and the S_γ of Cys 167 occupies a position different than the hydroxyl present in the wild type.

Derivatization of Sulfhydryl Groups. During the investigation, it became apparent that the mutant enzymes are prone to oxidation despite the presence of 20 mM 2-ME in the crystallization medium. It was noticed that some cysteines in the crystals were modified to form *S*,*S*-(2-hydroxyethyl)-thiocysteine, presumably by reacting with 2-hydroxyethyl disulfide, the product of oxidation of mercaptoethanol (2-ME). Although disorder may contribute to the spread of electron density, leading to difficulty in assessment of cysteine derivatization, density maps were analyzed at very low contouring levels to lower the probability of misinterpreting such situations (Figure 3). The state of all cysteine residues in the structures is summarized in Table 6. Cys 161 was not modified in any crystal examined, presumably because it is completely buried in a hydrophobic environment lined by four Phe, three Leu, two Val, one Trp, and one Tyr residue (Figure 4). The tight packing reduces the likelihood of disorder in this region and makes it virtually certain that there is no chemical modification present. Three of the five cysteine residues in S167A were derivatized. Unexpectedly, the catalytic cysteine, Cys 146, is apparently not derivatized. There is evidence for disorder of its S_γ (vide supra), which may reflect partial thiolation, but the major conformer has

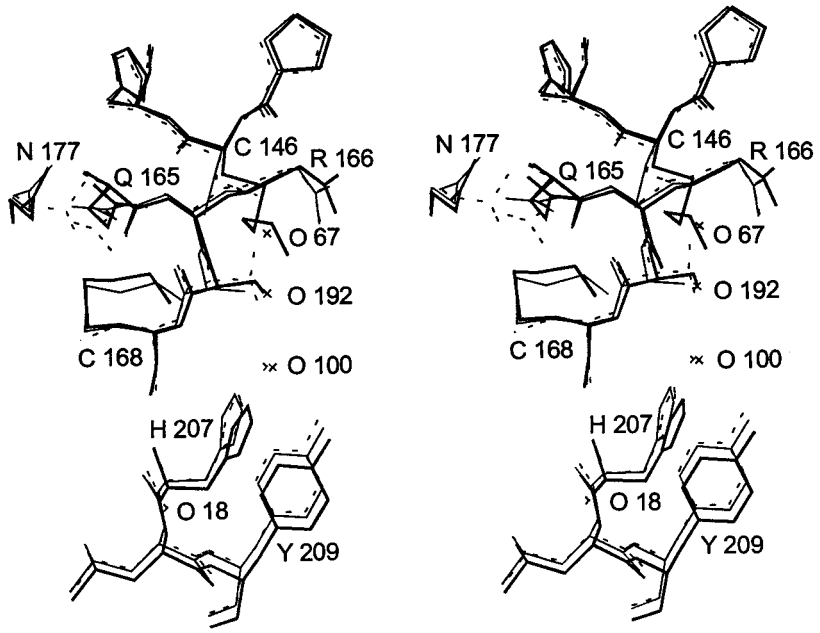

FIGURE 2: Superposition of the structures of ecTS S167T-"reduced" (dashed line), S167C (thick dark line), and S167A (thin line). The conformation of Cys 146 in S167T-"reduced" is identical to that in wild-type TS (PDB code 1tjs; *17*).

no additional density. The catalytic cysteines in S167T and in S167C were oxidized. The engineered Cys 167, positioned next to Cys 146, was neither derivatized nor bound to Cys 146. The state of Cys 192 in crystals of S167C is uncertain; it is likely to be derivatized and disordered but the electron density is inconclusive due to the lower resolution of the data.

To investigate further the modification of cysteine residues, attempts were made to reverse their derivatization in crystals of S167T, which were from the same batch that was used for structural analysis. Fresh 2-ME was added to the well solution every 4 days for 3 weeks. Prior to mounting, the crystal was transferred to a stabilizing solution containing 20 mM fresh 2-ME and then to a cryoprotectant, which also contained fresh reducing agent. The electron density maps for reduced S167T showed that the modification of Cys 146 and Cys 168 was reversed, while Cys 50 and Cys 192 remained derivatized.

Superpositions of Structures. In general, the coordinates and temperature factors of the TS models reported here are in excellent agreement. We used as the reference the model of S167A, which was refined first. The rms deviations of the positions of C_α between the reference and S167T, S167T-"reduced", S167C, and wild-type TS (PDB code 1tjs; *17*) were 0.12, 0.17, 0.47, and 0.35 Å respectively (Figure 2). The superposition of S167T and S167T-"reduced" yielded an rms deviation of 0.17 Å, indicating that the derivatization of the sulfhydryl groups with 2-ME had only a minor effect on the overall TS structure.

DISCUSSION

The binding of dUMP and CH_2H_4folate to TS causes a major conformational change, which converts the enzyme from an open form to a closed form of the ternary complex (*26*). This is followed by the rate-limiting step of chemical transformation of enzyme-bound substrate to enzyme-bound product. Analysis of the transient state of ternary complex formation was employed to assess the effect of substitution at Ser 167 on the rate of isomerization and the chemical transformation reaction steps. The forward rate of isomerization (k_{iso}) was shown to be moderately decreased (1.1−8.0-fold) by substitution at residue 167, with negligible effect on the reverse rate of isomerization ($k_{r,iso}$). The K_d(CH_2H_4-folate) for initial binding was increased slightly (<1.5-fold) for the mutant enzymes; however, the K_d for productive binding was increased significantly, results that are consistent with K_m values determined by steady-state analysis of Ser 167 mutants. The mutation at position 167 of ecTS lowered the rate-limiting step of chemical transformation (k_{chem}) by 1.1-, 5-, and 6-fold for S167A, S167G, and S167T, respectively). These values parallel the values of k_{cat} observed for the mutant enzymes in steady-state analysis.

The hydroxyl group of highly conserved Ser 167 of *E. coli* TS (Ser 216 of hTS and Ser 219 of lcTS) forms one of seven hydrogen bonds to the phosphate group of dUMP (*3*, *23*). The lack of activity of TSs with aspartate, asparagine, valine, and leucine substitutions at this position in growth complementation analyses may be due to the larger volume of their side chains. A large side-chain volume at this position may cause steric hindrance that disables substrate binding or reorients ligands in the active site. More interesting are mutants with small side chains (Ala, Gly, Thr, and Cys), which conferred thymidine prototrophy and produced catalytically active TS. For the most active mutant, S167A, the k_{cat} is reduced by a factor of 1.1 and the K_m for dUMP is increased approximately 5-fold. This mutant protein is a very efficient enzyme in which only the binding of dUMP is affected by the elimination of one enzyme−substrate hydrogen bond. S167G is significantly less active than S167A, with k_{cat}/K_m for dUMP decreased by 30-fold, relative to S167A. Differences in the solvent structure in the mutant proteins are likely to be responsible for the different kinetic parameters of S167A and S167G, since unfavorable interactions between the substrate and side chain of 167 are not a factor. The requirements on the volume of the side chain at position 167 are apparently more stringent for the partial than

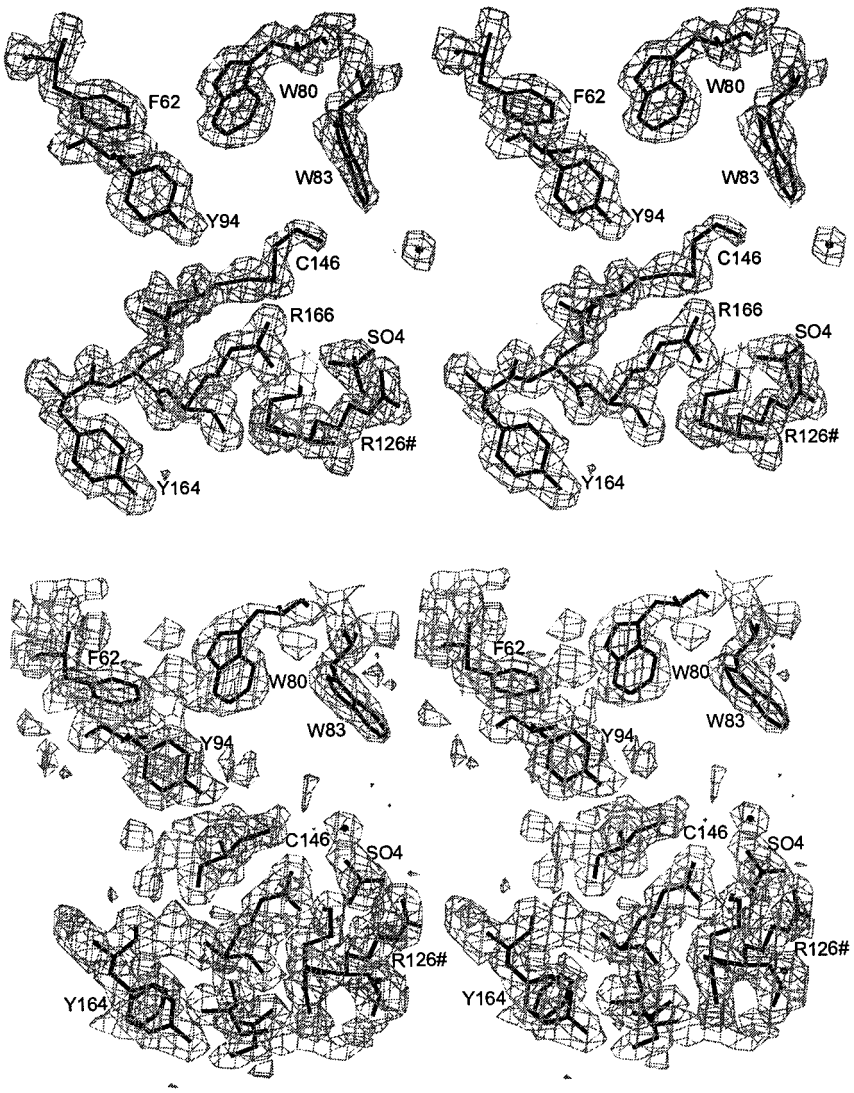

FIGURE 3: Electron density for the active-site Cys 146 in the ecTS S167T: (top) standard form and (bottom) "reduced" crystals. The contouring levels are 1.2σ (top) and 1.0σ (bottom). The $2F_o-F_c$ density map of S167T-"reduced" is drawn at a relatively low contouring level and a high coverage (2.0 Å). It shows that the catalytic cysteine is not derivatized with 2-mercaptoethanol as in the top panel, while the noise of the map starts to show.

Table 6: State of Derivatization of Cysteine Residues in Ser167 Variant TSs

	residue number					
enzyme	Cys 50	Cys 146	Cys 161	Cys 167	Cys 168	Cys 192
Ala167	yes	no	no	NP[a]	yes	yes
Thr167	yes	yes	no	NP	yes	yes
Thr167 (red)	yes	no	no	NP	no	yes
Cys167	yes	yes	no	no	yes	?

[a] NP, not present.

the complete TS reaction, as S167A and S167G, but not S167T and S167C, were active in the dehalogenation of BrdUMP. This may be due to the larger size of the Br subsituent versus H, which may make steric effects more critical.

In a previous investigation, 12 mutant hTSs were created with substitutions at the position corresponding to 167 in ecTS (216 in hTS) (*5*). As observed with ecTS mutants, hTS mutants with large side-chain volumes at position 216 (S216D, S216N, S216V, S216H, S216L, S216M, and S216Y) were unable to complement thymidine auxotrophy in TS-deficient bacteria. In contrast, marked species differences in behavior are observed between mutant proteins with alanine and threonine substitutions. S216A exhibited very low catalytic activity, only 1% that of wild-type enzyme, and was unable to complement the growth of TS-deficient bacteria at levels of expression of 5−6% (*5*). S216T exhibited 50% of the catalytic activity of wild-type hTS, while S167T exhibited only 15% of the catalytic activity of wild-type ecTS. The K_m values for dUMP of S216T and S167T were increased by 1.6- and 38-fold, respectively, relative to the wild-type enzymes.

dUMP binds to TS in a highly constrained orientation. When other side chains replace the side chain of Ser 167, dUMP loses one hydrogen bond and becomes more dependent on cofactor binding. Not surprisingly, k_{cat}/K_m values for dUMP were significantly decreased (5−9000-fold) for the mutant enzymes. In addition, K_ms for CH_2H_4folate were moderately increased (1.4−16-fold) for the mutant enzymes, indicating that substitution at position 167 affects the binding of CH_2H_4folate. Since bound dUMP forms the binding surface against which the pterin ring of the cofactor binds,

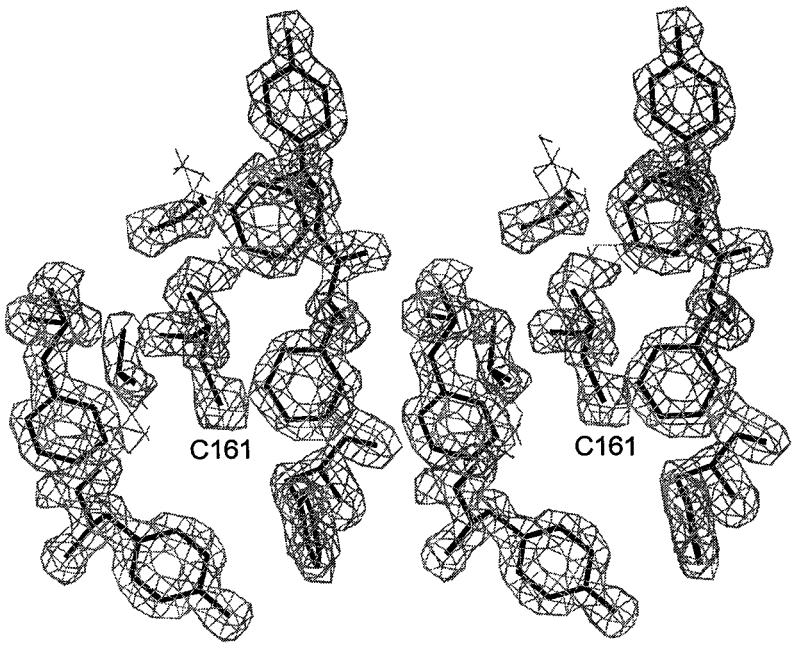

FIGURE 4: Environment of Cys 161, which is resistant to oxidation. The electron density map is at 2.0σ level.

lack of restraint on dUMP binding may result in slightly higher K_m values for cofactor (*3*, *23*).

Titration of enzymes with DTNB provides an estimate of the number of sulfhydryl groups undergoing oxidation but not their identity. Our serendipitous finding that 2-ME used during purification and crystallization derivatized cysteine residues to different extents provided insight into this process. Variation in experimental conditions may play a role in cysteine oxidation during the crystallization process. The time interval between protein purification and X-ray data collection was not constant, and oxygen diffusion to the crystals was not monitored. Therefore we examined the differences between derivatization of cysteine residues within each crystal separately. Solvent accessibility plays a crucial role in susceptibility of cysteine residues to oxidation, as indicated by the observation that the buried Cys 161 is not derivatized in the structures reported here. The other cysteine residues are reactive and tend to undergo oxidation. Unexpectedly, the active-site cysteine does not appear to be more reactive than the other exposed sulfhydryls. To the contrary, in the S167A mutant and in the "reduced" S167T it was not derivatized, and it did not form a disulfide bond with nearby Cys 167 in the S167C mutant (Figure 3, bottom). This indicates that the protonated state of the thiol of Cys 146 is favored in crystals of the apoenzyme. This is consistent with the measured pK_a of 8.0 for the catalytic cysteine lcTS (*27*), a value not much different from the average.

Since the residues in the active site of TS are highly conserved, it appears likely that the different response to the mutations in this site in ecTS and hTS are mediated by structured water molecules in the active site. Unfortunately, unliganded hTS crystallizes in inactive conformation with residues 181−197, corresponding to ecTS 132−148, in very different positions (*28*), which makes comparisons of the solvent structure in the active site not entirely relevant. In the S167A mutant, there are three water molecules, Wat67, Wat192, and Wat100, that connect the catalytic Cys 146 to His 207 through a chain of hydrogen bonds (Figure 1). Wat100, next to His 207 (2.9 Å) and Tyr 209 (3.1 Å), is conserved in the structures of all mutants reported here except S167C, which has poor solvent structure. Its position corresponds to the position of the 3′ OH substitutent of dUMP in binary and ternary complexes. Wat192 is present in wild-type ecTS and S167A, but in the other structures, 2-ME attached to Cys 146 occupies its position. We propose that this chain functions as a "proton wire" that facilitates the activation of Cys 146. The N_δ of His 207 is within hydrogen-bonding distance, 2.8−3.2 Å, of the carboxylate of Asp 205. The diad is polarized and the N_ϵ of the imidazole tends to be strongly basic. In apo-TS, this basicity is reduced by the charge of the guanidinium moiety of Arg 126′ (from the other subunit), which is stacked against the imidazole. Upon dUMP binding, the guanidinium binds to the phosphate and its charge is neutralized. This should reduce the electrostatic effect on the imidazole, increase the basicity of His 207, and trigger proton abstraction from Cys 146. It is likely that in wild-type TS, the hydroxyl of Ser 167 is involved in the proton transfer either directly or through ordering of the solvent. It should be emphasized that this hypothesis is based on the assumption that the process of substrate binding starts with phosphate attachment, since the space occupied by water molecules in the active site is occupied by ligands in the ternary inhibitory complex. The advantage of a system in which substrate binding triggers the detachment of the proton from Cys 146 is that the apoenzyme is less prone to oxidation. This phenomenon may account for the lack of apparent oxidation of Cys 146 in crystals of S167A, the mutant protein exhibiting the highest catalytic activity. In summary, a possible explanation of the kinetic data is that small side chains at ecTS position 167 are able to accommodate a network of water molecules in the active site that allows proton transfer and activation of the catalytic sulfhydryl.

REFERENCES

1. Perry, K. M., Fauman, E. B., Finer-Moore, J. S., Montfort, W. R., Maley, G. F., Maley, F., and Stroud, R. M. (1990) *Proteins: Struct., Funct., Genet. 8*, 315−333.

2. Finer-Moore, J. S., Fauman, E. B., Foster, P. C., Perry, K. M., Santi, D. V., and Stroud, R. M. (1993) *J. Mol. Biol. 232*, 1101−1116.
3. Finer-Moore, J. S., Montfort, W. R., and Stroud, R. M. (1990) *Biochemistry 29*, 6977−6986.
4. Hoganson, D. K., Williams, A. W., and Berger, S. H. (1999) *Biochem. Pharmacol. 58*, 1529−1537.
5. Williams, A. W., Dunlap, R. B., and Berger, S. H. (1998) *Biochemistry 37*, 7096−7103.
6. Ho, S. N., Hunt, S. D., Horton, R. M., Pullen, J. K., and Pease, L. R. (1989) *Gene 20*, 51−59.
7. Ellis, R. J., Van der Vies, S. M. (1991) *Annu. Rev. Biochem. 60*, 321−347.
8. Dunlap, R. B., Harding, N. G. L., and Huennekens, F. M. (1971) *Biochemistry 10*, 88−97.
9. Ellis, K. J., and Morrison, J. F. (1982) *Methods Enzymol. 87*, 405−426.
10. Zapf, J. W., Weir, M. S., Emerick, V., Villafranca, J. E., and Dunlap, R. B. (1993) *Biochemistry 32*, 9274−9281.
11. Garrett, C., Wataya, Y., and Santi, D. V. (1979) *Biochemistry 18*, 2798−2804.
12. Spencer, H. T., Villafranca, J. E., and Appleman, J. R. (1997) *Biochemistry 36*, 4212−4222.
13. Ellman, G. L. (1959) *Arch. Biochem. Biophys. 82*, 70−77.
14. Bradshaw, T. P., and Dunlap, R. B. (1989) *Biochim. Biophys. Acta 165*, 1163.
15. McPherson, A. (1990) *Eur. J. Biochem. 189*, 1−23.
16. Otwinowski, Z., and Minor, W. (1997) *Methods Enzymol. 276*, 307−326.
17. Stout, T. J., Sage, C. R., and Stroud, R. M. (1998) *Structure 6*, 839−848.
18. Navaza, J. (1994) *Acta Crystallogr. A50*, 157−163.
19. Collaborative Computational Project, Number 4 (1994) *Acta Crystallogr. D50*, 760−763.
20. Lamzin, V. S., and Wilson, K. S. (1993) *Acta Crystallogr. D49*, 129−147.
21. Brunger, A. T., Adams, P. D., Clore, G. M., Delano, W. L., Gros, P., Grosse-Kunstleve, R. W., Jiang, J.-S., Kuszewski, J., Nilges, M., Pannu, N. S., Read, R. J., Rice, L. M., Simonson, T., and Warren, G. L. (1998) *Acta Crystallogr. D54*, 905−921.
22. Sack, J. S., and Quiocho, F. A. (1997) *Methods Enzymol. 277*, 158−173.
23. Matthews, D. A., Appelt, K., Oatley, S. J., and Xuong, N. H. (1990) *J. Mol. Biol. 214*, 923−936.
24. Finer-Moore, J. S., Liu, L., Schafmeister, C. E., Birdsall, D. L., Mau, T., Santi, D. V., and Stroud, R. M. (1996) *Biochemistry 35*, 5125−5136.
25. Montfort, W. R., Perry, K. M., Fauman, E. B., Finer-Moore, J. S., Maley, G. F., Hardy, L., Maley, F., and Stroud, R. M. (1990) *Biochemistry 29*, 6964−6977.
26. Carreras, C. W., and Santi, D. V. (1995) *Annu. Rev. Biochem. 64*, 721−762.
27. Munroe, W. A., Lewis, C. A., Jr., and Dunlap, R. B. (1978) *Biochem. Biophys. Res. Commun. 80*, 355−360.
28. Schiffer, C. A., Clifton, I. J., Davisson, V. J., Santi, D. V., and Stroud, R. M. (1995) *Biochemistry 34*, 16279−16287.

BI000367G